THE JOURNAL OF PHYSICAL CHEMISTRY A

Article

pubs.acs.org/JPCA

How Many Chiral Centers Can Raman Optical Activity Spectroscopy Distinguish in a Molecule?

Benjamin Simmen, Thomas Weymuth, and Markus Reiher*

Laboratorium für Physikalische Chemie, ETH Zurich, Wolfgang-Pauli-Strasse 10, 8093 Zurich, Switzerland

Supporting Information

ABSTRACT: To study the capabilities and limitations of Raman optical activity, (−)-(*M*)σ-[10]helicene and (−)-(*M*)σ-[4]helicene serve as scaffold molecules on which new chiral centers are introduced by substitution of hydrogen atoms with other functional groups. These functional groups are deuterium atoms, fluorine atoms, and methyl groups. Multiply deuterated species are compared. Then, results of singly deuterated derivatives are compared against results obtained from singly fluorinated and methylated derivatives. The analysis required the calculation of a total of 2433 Raman optical activity spectra. The method we propose for the comparison of the various Raman optical activity spectra is based on the total intensity of squared difference spectra. This allows a qualitative comparison of pairs of Raman optical activity spectra and the extraction of the pair of most similar Raman optical activity spectra for each group of stereoisomers. Different factors were accounted for, such as the spectral resolution (modeled by line broadening) and the range of vibrational frequencies considered. In the case of σ-[4]helicene all generated stereoisomers in each group can be distinguished from one another by Raman optical activity spectroscopy. For σ-[10]helicene this holds except for the lower one of the two resolutions considered. Here, the group consisting of stereoisomers with five chiral centers contains at least one pair of derivatives whose Raman optical activity spectra cannot be distinguished from one another. This indicates that an increased molecular size has a negative effect on the number of chiral centers which can be distinguished by Raman optical activity spectroscopy. Regarding the different substituents, stereoisomers are the better distinguishable in Raman optical activity spectroscopy, the more distinct the signals of the substituent are from the rest of the spectrum.

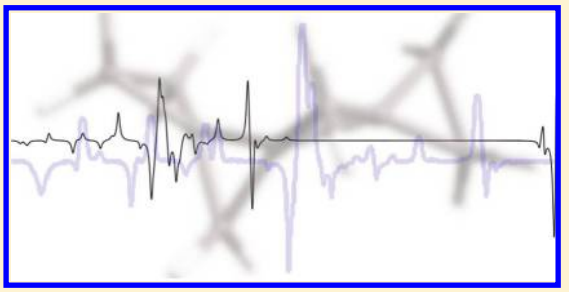

1. INTRODUCTION

The absolute configuration of a molecule is often decisive for its function. For instance, biochemical activity heavily depends on the absolute configuration. One example is carvone, which in its D-form smells like spearmint, while its L-form smells like caraway.[1] Synthetic tools for controlling the stereochemistry have been continuously developed over past decades, allowing chemists to synthesize a large number of molecules in enantiomerically pure forms.[2]

Even though the principles of chirality were already known at the end of the 19th century, structural analysis is still a challenging task when it comes to the determination of absolute configuration. For molecules containing only one chiral center this task is already not trivial, and it gets rapidly more difficult with an increasing number of chiral centers, since a molecule with N chiral centers has 2^N different possible stereoisomers.

The stereochemistry of a molecule can be determined by X-ray diffraction experiments. Although this allows one to determine the absolute configuration within a crystal structure, it has several considerable disadvantages. The main disadvantage is the fact that the substance has to be in crystalline form of a sufficient amount. This is not always possible, especially not for large biomolecules or expensive molecules. It is difficult if not impossible to analyze dynamic systems (e.g., solutions) and the technique is insensitive to light atoms such as hydrogen (which could be solved by neutron scattering).

The application of optical activity in the study of stereochemistry has recently experienced a renaissance.[3] For a long time it was only possible to observe optical activity due to electronic excitations. The vibrational form of optical activity,[4] however, holds promises of greater practicality due to an increased number of signals within a spectrum; i.e., it provides more information. The increased amount of information stems from the fact that it is possible to excite more degrees of freedom of the molecule under study.

Since there are two fundamental types of vibrational spectroscopy, i.e., infrared absorption based (IR) and scattering Raman spectroscopy, both routes were pursued to detect vibrational optical activity.[5] Although first experiments were performed as early as 1930 by Kastler[6] and also by Bhagavantam and Venkateswaran,[7] Barron et al. were the first to accomplish Raman optical activity (ROA) scattering measurements in 1973,[8] two years after formulating the theory of ROA scattering.[9] The results of Barron et al. were confirmed by Hug et al. two years later in 1975.[10] ROA spectroscopy

Received: April 10, 2012
Revised: May 14, 2012
Published: May 24, 2012

measures the difference of right and left circularly polarized light. Although some time has passed since the first successful experiment, ROA has only recently become a standard probing technique.[3,5,11] This is due to a much lower signal-to-noise ratio than its IR counterpart called "vibrational circular dichroism" (VCD).[12] The introduction of the backscattering setup,[13] which nowadays is the most common way to perform this kind of experiment, was a breakthrough and finally gave satisfactory results. It should be noted that ROA has some advantages over VCD. The most important one is its capability of allowing spectra to be recorded in aqueous solutions, thus allowing analysis of biomolecules and even viruses[14] under natural conditions.

Even though measuring an ROA spectrum is now routine for small molecules, its interpretation is still a challenge, since no direct relation between the signal pattern and the molecular structure is available. Methods from theoretical chemistry allow one to assign ROA spectra for molecules of medium size: polymers,[15−17] mono-, di-, and polypeptides,[18−28] transition metal complexes,[29−32] carbohydrates,[33−35] organic molecules,[36−49] and biochemical systems.[50−53] Theoretical approaches proved to be very reliable so that predictions are feasible.[29,30] Theoretical studies of molecules with several hundred atoms and even small proteins[52] have become possible. The standard approach[54] can be supplemented by more approximate schemes[41] if certain caveats are taken into account.[55−57]

Theoretical methods are often applied to assign the fingerprint region of the measured spectra which allows for the assignment of the absolute stereochemistry. This task becomes more difficult with an increasing number of chiral centers and molecular size and eventually fails.[58] It is now at the heart of this work to explore the capabilities and limits of ROA spectroscopy for highly complex stereoisomers. The aims of this work are first to determine the largest number of chiral centers which ROA can detect in a molecule and second to assess how different factors affect the capability of ROA spectroscopy to detect chiral centers formed by different functional groups. This is achieved by selecting two scaffold molecules into which new chiral centers are introduced. These stereoisomers will be grouped according to their number of chiral centers N. The pair of structures with the most similar ROA spectra will be identified in each group. The ROA spectra of this pair of stereoisomers will then be analyzed visually with respect to their distinguishability. If the spectra are distinguishable, it is concluded that all other pairs of ROA spectra in this group are also distinguishable since they are less similar. If the identified pair of ROA spectra is found to be indistinguishable, further analysis of higher substituted derivatives is stopped, since it is already in the group under consideration not possible to distinguish all ROA spectra from one another.

This work is organized as follows. First, in section 2 the computational methodology and in section 3 the scaffold molecules into which the chiral centers are introduced are described. Then, the measure of similarity is introduced in section 4. Next, the results of the multiply deuterated derivatives of the scaffold molecule are presented in section 5. Furthermore, we present the results from the analysis of different substituents. The paper concludes in section 6 with a general discussion.

2. COMPUTATIONAL METHODOLOGY

Structure optimizations were performed with the parallelized version of the TURBOMOLE package 6.0.2.[59] The density functional theory (DFT) calculations were performed with the resolution of the identity (RI) density-fitting approximation utilizing the BP86 exchange−correlation functional.[60,61] The basis set chosen was def-TZVPP (Ahlrichs' valence triple-ζ basis set with two sets of polarization functions)[62,63] on all atoms. The auxiliary basis set was chosen accordingly.[64,65] The Cartesian coordinates of all optimized structures are presented in the Supporting Information (the two unsubstituted scaffold molecules, the four methylated derivatives, and the four fluorinated derivatives).

The vibrational frequencies and ROA backscattering intensities (i.e., derivatives of the property tensors with respect to the normal modes) were calculated seminumerically with the SNF program[66] using a local version of TURBOMOLE[29] for the calculation of the ROA property tensors. The difference quotients required to approximate the analytic derivatives were determined with a three-point central difference formula by distorting the Cartesian coordinates of the nuclei individually with a step size of ± 0.01 bohr in all three dimensions, resulting in six distortions per atom. The analytic energy gradients required for the vibrational frequencies were obtained with the TURBOMOLE package. The harmonic vibrational frequencies obtained with BP86 and a triple-ζ basis set are often close to the experimentally measured fundamental ones[67−70] due to a fortunate error cancellation effect.[71] Hence, they have not been scaled.

As already mentioned, the property tensors required for ROA spectra were obtained with a local version[29] of the ESCF[72] module from the TURBOMOLE package (version 5.7.1). The velocity representation was chosen for the electric-dipole operator to ensure gauge invariance. The excitation wavelength was set to 798 nm (which corresponds to the frequency of a Ti:Al_2O_3 laser[73]). By applying time-dependent DFT, it was verified that all singlet and triplet excitations have excitation wavelengths which are significantly below this value. The singlet and triplet excitation energies were calculated with the TURBOMOLE package employing the same method as for the structure optimizations.

Analysis of squared difference spectra was carried out with custom-made Perl scripts. Plotting of spectra and statistical analysis were carried out with the R[74] environment together with its Cairo Package[75] and Inkscape.[76] Three-dimensional molecular structures were depicted with Avogadro.[77]

It is clear that the spectral resolution will have a rather large impact on the distinguishability of a given pair of spectra. Therefore, in this work we employ (artificial) line broadening (with Lorentzian line shapes) to model a finite resolution. We can then characterize the spectral resolution as the full width at half-maximum (fwhm) of the broadened lines. To ensure that a wide enough range of resolutions is considered, the analysis is performed with two fwhm values separately. The fwhm corresponding to a lower resolution is set to 20 cm^{-1}, whereas the fwhm corresponding to a higher resolution is set to 7 cm^{-1}.

3. CHOICE OF SCAFFOLD MOLECULES

If one wants to determine the largest number of chiral centers which ROA spectroscopy can detect in a molecule, a considerable number of stereoisomers is required. They are most easily obtained by introducing new chiral centers into a

dx.doi.org/10.1021/jp303428f | J. Phys. Chem. A 2012, 116, 5410−5419

scaffold molecule, by for instance substituting atoms/functional groups by other atoms/functional groups. An appropriate scaffold molecule suited for an efficient generation of these stereoisomers is bound to fulfill several requirements. For instance, the molecule should be apolar so that solvation effects can be expected to be described properly by a dielectric screening model or may even be completely neglected as in this work. Also, new chiral centers should be introduced systematically and not disturb the original structure. The last requirement is a large ratio between the number of possible new chiral centers and the number of atoms in the molecule, if one wants to perform an efficient analysis. For these reasons, we chose as scaffold molecules from which the stereoisomers are generated (−)-(*M*)σ-[4]helicene and (−)-(*M*)σ-[10]-helicene (from here on denoted simply as σ-[4]helicene and σ-[10]helicene). Figure 1 depicts the structures of the two scaffold molecules.

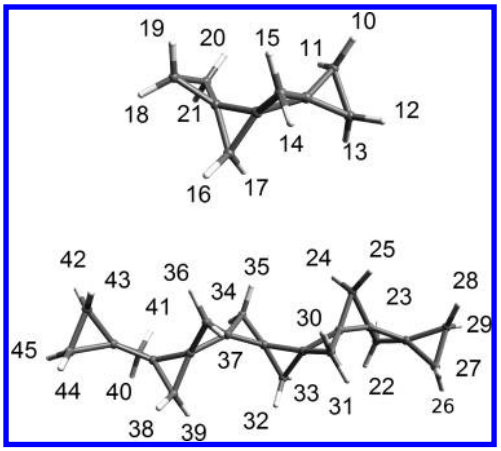

Figure 1. Structures of the two scaffold molecules σ-[4]helicene (top) and σ-[10]helicene (bottom). The numbers distinguish the hydrogen atoms. Substitution patterns are in general formulated through listing the numbers of those hydrogen atoms which have been substituted. The numbers also indicate the line numbers in their corresponding Cartesian coordinate files which are presented in the Supporting Information.

The term "σ-[*n*]helicenes" was coined by de Meijere[78] and relates to a special, nonbranched and acyclic form of triangulanes which are a subspecies of spiro compounds.[79] The *n* indicates the number of triangulane elements the molecule is built of. The name refers to its similarity to π-[*n*]helicenes, but instead of being aromatic, the structure consists solely of σ-bonds. Helicenes with $n > 3$ are chiral with respect to their sense of rotation (axial chirality).[79] Enantiomerically pure synthesis has been reported for $n \leq 7$.[80] Additionally, Hug and co-workers have already illustrated the accuracy of calculated ROA spectra for (−)-(*M*)σ-[4]helicene.[37] Figure 2 depicts the experimental ROA spectrum of (−)-(*M*)σ-[4]helicene from Hug and co-workers[37] together with our theoretical spectrum. The clear visual similarity serves as our starting point.

This work focuses on stereoisomers which are generated by replacing at most one hydrogen atom per carbon atom by a deuterium atom. These stereoisomers will be denoted as "deuterated derivatives" of the scaffold molecules. The advantage of introducing new chiral centers by isotopic substitution is that the new structures do not have to be optimized again; i.e., the same atom positions can be used as

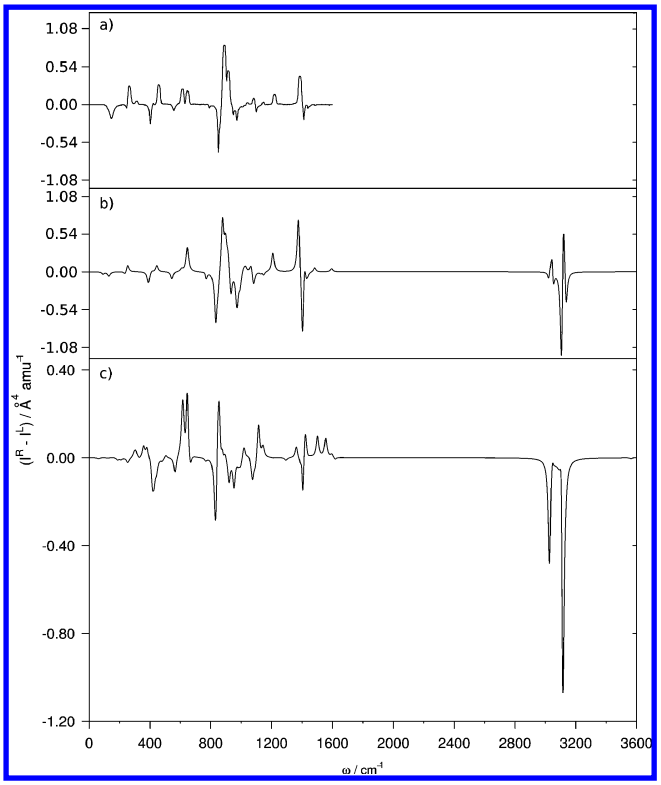

Figure 2. Experimental spectrum (a) from Hug and co-workers[37] of (−)-(*M*)σ-[4]helicene compared with our calculated spectra of (−)-(*M*)σ-[4]helicene (b) and (−)-(*M*)σ-[10]helicene (c). Both calculated spectra have been broadened with Lorentzians with a fwhm of 20 cm^{-1}.

the potential energy surface remains the same (within the Born−Oppenheimer approximation it is not dependent on the mass of isotopes). Also, the property tensors and the (non-mass-weighted) Hessians of the two scaffold molecules do not change and can thus be reused. The chiral information solely enters the spectrum calculation through the mass-weighted normal coordinates which enter the property derivatives.

In its unsubstituted form, each hydrogen atom in a σ-[*n*]helicene has one other homotopic hydrogen atom due to the C_2 symmetry of the molecule. A table listing the equivalent hydrogen atoms for both scaffold molecules is presented in the Supporting Information. Because of this, the maximum number of possible chiral centers is the number of triangulane elements *n* plus 2. For example, for σ-[10]helicene this number is 12. Each hydrogen atom in the two scaffold molecules has a unique index, so it can easily be stated which hydrogen atoms have been replaced in a certain derivative. Figure 1 shows the indices of the hydrogen atoms which will describe the substitution pattern of the scaffold molecule derivatives. Note that the atom labels are the same as the indices used in the Cartesian coordinates of the structures presented in the Supporting Information.

For the analysis of σ-[4]helicene all possible deuterated stereoisomers are generated. The number of derivatives N_{Der} which are generated depends on the number of triangulane elements *n* and the number of chiral centers *N*. For even *n* we have the expressions

dx.doi.org/10.1021/jp303428f | J. Phys. Chem. A 2012, 116, 5410−5419

$$N_{\mathrm{Der}} = \begin{cases} \frac{1}{2}\left(2^N \binom{n+2}{N}\right) & \text{if } N \text{ is odd} \\ \frac{1}{2}\left(2^N \binom{n+2}{N} + 2^{N/2}\binom{(n+2)/2}{N/2}\right) & \text{if } N \text{ is even} \end{cases} \quad (1)$$

for calculating the number of derivatives. The reason why we have to distinguish between the cases where N is either even or odd is the symmetry of the molecule. The C_2 symmetry of the molecule results in a homotopic partner for each hydrogen atom. Since we have an even value for n in both cases, the symmetry is always broken if an odd number of stereocenters is introduced. If an even number of stereocenters is introduced, it is possible that the symmetry is conserved. This will always be true if both hydrogen atoms of a homotopic pair are substituted. If we would apply the formula for odd N to the case of an even N, we would only count half of the symmetrically substituted derivatives.

However, for σ-[10]helicene it is not feasible to generate all deuterated isostereomers as for σ-[4]helicene since the number of spectral comparisons is too large. Thus, in the case of σ-[10]helicene the number of carbon atoms considered as a position for substitution is equal to the number of new chiral centers. For singly deuterated derivatives of σ-[10]helicene only hydrogen atom 22 or 23 have been substituted, whereas in the case of doubly deuterated derivatives of σ-[10]helicene either hydrogen atom 22 or 23 and either hydrogen atom 24 or 25 has been substituted. This results in fixed positions of the chiral centers in the scaffold molecule. To be able to compare the results of σ-[10]helicene to the ones of σ-[4]helicene, the corresponding subset of deuterated derivatives of σ-[4]helicene is selected from the full set. Thus, in this comparison, the singly deuterated derivatives of σ-[4]helicene are only substituted in either position 10 or 11. The doubly deuterated derivatives of σ-[4]helicene can be substituted in either position 10 or 11 and either position 12 or 13. All further derivatives are generated accordingly. Thus, the number of derivatives in each group is 2^N except if $n + 2 = N$. Here, eq 1 holds again.

For a further analysis, also methylated and fluorinated derivatives are generated. However, here the Hessians and the property tensors of the scaffold molecules have to be recalculated for the derivatives. Thus, only singly methylated and singly fluorinated derivatives are generated and the results are qualitatively compared to the ones obtained from the deuterated derivatives. The generated stereoisomers are substituted in either position 10 or 11 for σ-[4]helicene and in either position 22 or 23 for σ-[10]helicene. In total, this work required the calculation of 2433 ROA spectra.

4. MEASURES TO ASSESS SPECTRA SIMILARITY

There are several possible ways to analyze the ROA spectra of the generated stereoisomers with respect to their distinguishability. We analyzed four different methods to find the most suited one for our work. One is based on simplified spectra, another one is based on a probabilistic description of the spectra, and two are based on a similarity measure.

In a first approach, the simplification of the ROA spectra is performed by transforming them into block spectra as proposed by Herrmann et al.[19] This simplification offers an important advantage, since for each pair of structures it is possible to clearly state whether their ROA spectra are different under the simplification of this scheme. However, when applied to our theoretical spectrum and the experimental spectrum of (−)-(*M*)σ-[4]helicene of Hug et al.,[37] this approach could not detect the visual similarity between the two spectra, which is the starting point of our analysis.

The second approach, which is based on a probabilistic description, takes into account that the vibrational frequencies of theoretical spectra contain a certain error. If one could estimate a suitable probability distribution of the vibrational frequencies, it would be possible to calculate the probability that all pairs of spectra in a group can be distinguished from one another by integration over the resulting multidimensional probability density. The advantage of this method is that it would give a very accurate description of the problem. Unfortunately, the computational requirements needed to evaluate the integration of the probability densities are extremely large for large data sets as employed in this study. Furthermore, it would be very difficult to obtain a reliable probability distribution function.

Approaches based on similarity measures do not allow for a direct conclusion of whether two spectra can be distinguished. However, they can be applied to extract the pair of spectra with the largest similarity. They thus allow us to determine whether all pairs of spectra in a group can be distinguished from one another based on the results of one pair of spectra. One such scheme was proposed and tested by Debie et al.[81] This scheme was originally developed for distinguishing enantiomers. It is based on a comparison of two spectra where only either positive or negative intensities are compared against each other, resulting in a similarity measure. This comparison is then performed once for the actual spectra and once with one spectrum inverted with respect to the sign of the intensities. The difference of the two similarity measures serves then as a confidence level.

The approach adopted in this work requires the calculation of the total intensity of the squared difference spectra for each pair of ROA spectra. In our approach, we take as a measure of the similarity of two spectra the square root of the total squared intensity difference ΔI^2 between the two spectra $f(\omega)$ and $g(\omega)$ with ω being the wavenumber. ΔI^2 is thus defined as

$$\Delta I^2 = \sqrt{\int_a^b (f(\omega) - g(\omega))^2 \, \mathrm{d}\omega} \quad (2)$$

with $a = 0$ cm^{-1} throughout this work. The value of b is chosen to take two values. The first value of $b = 1800$ cm^{-1} reflects the currently analyzed range of vibrational frequencies in ROA spectroscopy. The second value $b = 3600$ cm^{-1} includes all harmonic frequencies. The comparison of the results obtained from the two values of b will allow us to better understand the role of the functional group serving as a substituent. It is clear from eq 2 that ΔI^2 can be understood as the standard deviation from the case of completely identical ROA spectra.

Our approach then has two considerable advantages over the one proposed by Debie et al. The first advantage is that our approach is computationally much cheaper. The second advantage is that the differences between the similarity values produced by our approach are larger compared to the ones produced by the scheme of Debie et al.. This can be interpreted as a higher sensitivity to differences between the spectra.

Further advantages of our approach are that small differences are weighted less compared to larger differences because the difference between the spectra $f(\omega)$ and $g(\omega)$ is squared. If we

dx.doi.org/10.1021/jp303428f | J. Phys. Chem. A 2012, 116, 5410−5419

had taken the absolute of the difference, this would not be the case. Thus, we circumvent the problem that a large number of close-lying weak signals, which in practice would not be deemed distinguishable, could mathematically result in a large total difference if the absolute value was taken. Such problems are, however, a general issue with methods based on similarity measures.

It is important to note, since we compare only theoretical spectra, that we do not need to apply similarity measures that aim at a rather perfect match (for such a measure see ref 82).

The analysis of the deuterated derivatives of the scaffold molecules is then performed as follows. As mentioned above, the generated stereoisomers are grouped together according to their number of chiral centers. The similarity measure is then applied to the ROA spectra of all pairs of stereoisomers within one group. From all the calculated ΔI^2 values, the lowest ΔI^2 values within one group are extracted, and the spectra of the corresponding structures are plotted so that they can be analyzed visually. Thus only one pair of ROA spectra per group has to be compared. The pairs of spectra are considered distinguishable if they contain isolated signals (a signal is considered isolated if no other signal is adjacent such that small changes of wavenumber and/or intensity would lead to a superposition of the two) which have no counterpart in the other spectrum, or if the corresponding signals (signals with approximately the same vibrational frequency) have opposite intensities. If a pair of ROA spectra is deemed distinguishable, all other pairs of ROA spectra are also assumed to be distinguishable. If the pair of ROA spectra is considered nondistinguishable, we conclude that ROA spectroscopy is not capable of detecting the correct absolute configuration of all chiral centers in the stereoisomers in that group and the analysis is not carried out for higher substituted derivatives of that scaffold molecule. The analysis performed for the methylated and fluorinated derivatives is different. Since only singly methylated/fluorinated derivatives are generated, the resulting ΔI^2 values are compared against the ΔI^2 values of the singly deuterated derivatives.

5. RESULTS AND DISCUSSION

In this section we present the results of all analyzed cases. We start with the results of the complete set of deuterated derivatives of σ-[4]helicene. Then, we study the effect of the molecular size by making the transition from σ-[4]helicene to σ-[10]helicene. This requires selecting the appropriate subset of deuterated derivatives of σ-[4]helicene to compare with. To understand the differences between the subset and the complete set of deuterated derivatives of σ-[4]helicene, we compare the results obtained for set sizes first. In this way we are able to identify potential artifacts resulting from the restrictions imposed on the number of selected stereoisomers. Then we are prepared to compare the results of σ-[10]helicene to the corresponding ones of σ-[4]helicene. Finally, we discuss results of the singly substituted stereoisomers with different substituents.

5.1. Complete Set of Deuterated σ-[4]Helicene. Table 1 lists the lowest values of ΔI^2 for each group of σ-[4]helicenes characterized by the number of chiral centers N (for both resolutions and both values of the upper integration bound b considered). The corresponding ROA spectra and substitution patterns are presented in the Supporting Information. From Table 1 we see that the pairs of stereoisomers with the lowest ΔI^2 are always considered distinguishable. Notably, this is independent of both the value chosen for the fwhm and the value chosen for b.

Table 1. Results of the Complete Set of Multiply Deuterated Derivatives of σ-[4]Helicene[a]

		b = 1800 cm^{-1}		b = 3600 cm^{-1}		
N	fwhm	ΔI^2	Dst	ΔI^2	Dst	N_{Der}
1	20	0.005	yes	0.008	yes	6
2	20	0.005	yes	0.006	yes	33
3	20	0.005	yes	0.006	yes	80
4	20	0.004	yes	0.004	yes	126
5	20	0.005	yes	0.005	yes	96
6	20	0.005	yes	0.006	yes	36
1	7	0.013	yes	0.017	yes	6
2	7	0.013	yes	0.016	yes	33
3	7	0.010	yes	0.015	yes	80
4	7	0.012	yes	0.014	yes	126
5	7	0.011	yes	0.013	yes	96
6	7	0.013	yes	0.016	yes	36

[a]The minimal values of ΔI^2 (Å^4 amu^{-1}) are listed together with the information on whether the associated pair of stereoisomers is distinguishable (Dst) for all groups defined by their number of chiral centers (N). All results are listed for both values chosen for b and both values chosen for the fwhm (cm^{-1}). Last, the number of stereoisomers is listed for each group (N_{Der}).

Comparing the number of stereoisomers per group and the values of ΔI^2 in Table 1, we can see that an increase of the first usually results in a decrease of the latter. The number of stereoisomers is largest for N = 4 and second largest for N = 5. These are also the cases where ΔI^2 is the lowest. The number of structures is smallest for N = 1, where the values of ΔI^2 are the largest. From that we conclude that the number of stereoisomers which have to be considered affects the maximum number of chiral centers for which the absolute configuration can be detected.

Next, we investigate the influence of b. From Table 1 we see that the values of ΔI^2 increase when the value of b is chosen to be 3600 cm^{-1} instead of 1800 cm^{-1}. This is readily explained by the additional vibrational modes included in the analysis. Additionally, the maximum number of chiral centers for which the absolute configuration can be detected does not differ for the two chosen values of b. From this we assess that a relevant amount of chiral information is contained within the part of the spectrum where modes have vibrational frequencies lower than 1800 cm^{-1}. Since we chose deuterium atoms as substituents and since the C−D stretching modes have vibrational frequencies between 2200 and 2080 cm^{-1},[83] we confirm that chiral information is not limited to specific ranges of the spectrum. Due to vibrational modes which incorporate large parts of the spectrum (also the deuterium atoms), it is likely that the chiral information is spread over large parts of the spectrum.

5.2. Subset of Deuterated σ-[4]Helicene. Since it is not possible to analyze the same set of deuterated derivatives for σ-[10]helicene as has been done for σ-[4]helicene, we have to select the appropriate subset of deuterated derivatives as explained in section 3. However, if we compared these results to the ones obtained for σ-[4]helicene, we would not know whether the differences between the two results originated from the increased molecular size or from the different scheme used for generating the set of deuterated derivatives. Thus, we first have to analyze the subset of σ-[4]helicene and compare the

Table 2. Results of the Subsets of Multiply Deuterated Derivatives of σ-[4]Helicene and σ-[10]Helicene[a]

		σ-[10]helicene				σ-[4]helicene				
		b = 1800 cm^{-1}		b = 3600 cm^{-1}		b = 1800 cm^{-1}		b = 3600 cm^{-1}		
N	fwhm	ΔI^2	Dst	ΔI^2	Dst	ΔI^2	Dst	ΔI^2	Dst	N_{Der}
1	20	0.015	yes	0.025	yes	0.006	yes	0.017	yes	2
2	20	0.013	yes	0.021	yes	0.006	yes	0.015	yes	4
3	20	0.009	yes	0.019	yes	0.006	yes	0.008	yes	8
4	20	0.008	yes	0.017	yes	0.005	yes	0.006	yes	16
5	20	0.008	**no**	0.012	**no**	0.005	yes	0.005	yes	32
6	20					0.005	yes	0.006	yes	64
1	7	0.047	yes	0.058	yes	0.015	yes	0.028	yes	2
2	7	0.045	yes	0.055	yes	0.014	yes	0.025	yes	4
3	7	0.037	yes	0.049	yes	0.014	yes	0.016	yes	8
4	7	0.028	yes	0.044	yes	0.012	yes	0.015	yes	16
5	7	0.023	yes	0.034	yes	0.011	yes	0.014	yes	32
6	7	0.024	yes	0.034	yes	0.013	yes	0.016	yes	64
7	7	0.028	yes	0.032	yes					128
8	7	0.026	yes	0.031	yes					256
9	7	0.024	yes	0.025	yes					512
10	7	0.024	yes	0.025	yes					1024

[a]The minimal values of ΔI^2 (Å^4 amu^{-1}) are listed together with the information on whether the associated pair of stereoisomers is distinguishable (Dst) for all groups defined by their number of chiral centers (N). All results are listed for both values chosen for b and both values chosen for the fwhm (cm^{-1}). Last, the number of stereoisomers is listed for each group (N_{Der}).

results to the ones obtained for the complete set of deuterated σ-[4]helicene derivatives.

The results for the subset of deuterated derivatives are listed in Table 2 together with the results of the analysis of σ-[10]helicene. The corresponding ROA spectra and substitution patterns are presented in the Supporting Information. From the results for the subset of deuterated derivatives of σ-[4]helicene listed in Table 2, we draw the following conclusions. First, the absolute configuration of all chiral centers can always be detected. This is a direct consequence of the results listed in Table 1 since we study a subset of all deuterated derivatives of σ-[4]helicene.

Next, we compare the relations between the number of stereoisomers in a group and the respective value for ΔI^2 listed in Table 2. The largest number of stereoisomers is contained within the groups corresponding to N = 5 and N = 6. For N = 5 we also always find the lowest value of ΔI^2. Again, we can conclude that for the value of ΔI^2 there is some dependence on the number of stereoisomers considered. The increase of the value of ΔI^2 for N = 6, in comparison to N = 5, is likely to be an artifact from the scheme applied to generate the subset of deuterated derivatives.

As a next step, we analyze the influence of the value chosen for b. From Table 2 we notice that, as for σ-[4]helicene, the values of ΔI^2 increase if b is changed from 1800 to 3600 cm^{-1}. Again, this is readily explained by the additional modes included in the analysis and in complete agreement with the results obtained for the complete set of deuterated derivatives of σ-[4]helicene.

We thus conclude that the restrictions imposed on the selection of deuterated derivatives of σ-[4]helicene cause an increase of the values of ΔI^2 for some groups defined by N. Assessing how the maximum number of chiral centers for which the absolute configuration can be detected is affected by the restriction scheme is not possible since we did not observe any cases for which the absolute configuration was not detected. However, this has no serious implications: Every pair of structures in the subset of σ-[10]helicene which cannot be distinguished from one another by ROA spectroscopy is also contained within the complete set of structures. From this follows that the resulting minimal ΔI^2 of the complete set can only have a value equal to or lower than the one of the subset. Since the value of ΔI^2 is a measure of similarity and thus also a measure of distinguishability, we notice that it is not possible that the pair of structures of the complete set with a minimal value of ΔI^2 is better distinguishable than the ones from the subset. Hence, we will still be able to at least obtain an upper bound estimate for the number of chiral centers for which the absolute configuration can be determined by ROA spectroscopy.

5.3. Deuterated σ-[10]Helicene. Table 2 lists the results of σ-[10]helicene together with the results from the subset of σ-[4]helicene. The corresponding ROA spectra and substitution patterns are presented in the Supporting Information. First of all, we note that there are cases where the absolute configuration of all chiral centers cannot be unambiguously detected, namely for N = 5 and a value of 20 cm^{-1} chosen for the fwhm. Hence, taking into account the results from the analysis of the artifacts introduced by the restrictions imposed on the number of stereoisomers, we can conclude that N = 4 serves as our upper bound estimate for a fwhm of 20 cm^{-1}. Figure 3 illustrates the difference between a pair of spectra which is considered distinguishable and a pair of spectra which is considered indistinguishable. The value chosen for b does not affect the result. This agrees with our assessment from section 5.1, where we noticed that all relevant information is contained within the part having vibrational frequencies up to 1800 cm^{-1}. Since the absolute configuration can still be determined even if the C−D stretching vibration (in the range 2200−2080 cm^{-1} [83]) is *not* included in the analysis, other vibrational modes comprising the motion of the deuterium atom, such as scissoring or rocking modes, are decisive. These latter vibrations are highly delocalized, while the C−D stretching modes are the only localized modes contained in the molecules. Hence, delocalized vibrational modes are sufficient to

dx.doi.org/10.1021/jp303428f | J. Phys. Chem. A 2012, 116, 5410−5419

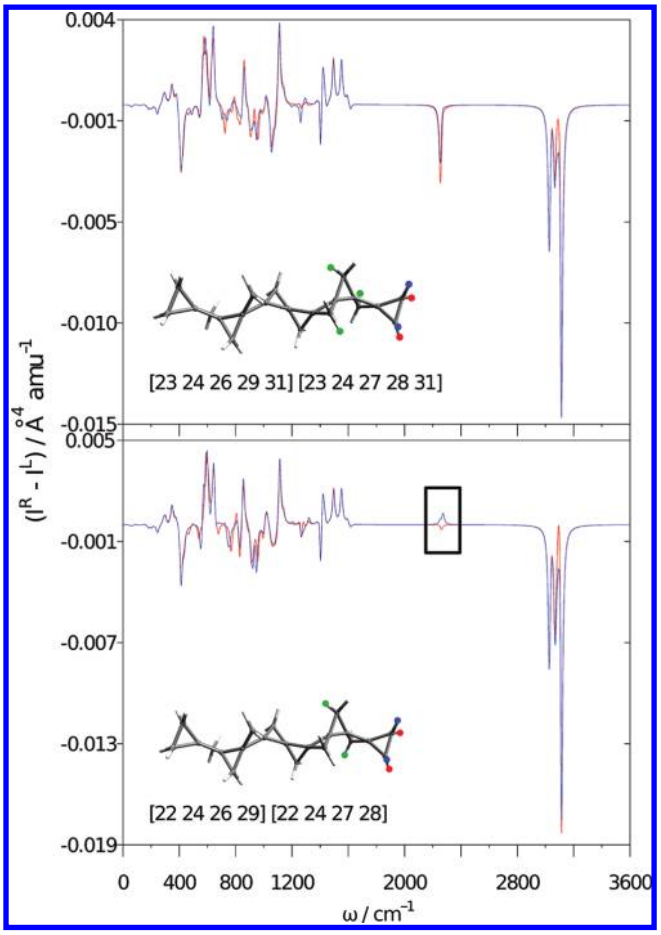

Figure 3. Pairs of ROA spectra which result in a minimal ΔI^2 for four times (bottom) and five times (top) deuterated σ-[10]helicene illustrating the difference between pairs of ROA spectra which are considered distinguishable (bottom) and indistinguishable (top) in this work. The pair of signals marked with a box (bottom) allows one to distinguish the two spectra. The fwhm and b are set to 20 cm^{-1} and 3600 cm^{-1}, respectively. The numbers in square brackets indicate the positions of deuteration of the studied derivatives. The structures associated with each plot illustrate the substitution pattern. Green dots specify positions deuterated in both stereoisomers, whereas the red and blue dots correspond to positions deuterated in only one of the stereoisomers. The red dots correspond to the red spectrum, whereas the blue dots correspond to the blue spectrum.

discriminate between two σ-[10]helicene spectra in ROA spectroscopy.

Next, we assess the relation between the number of stereoisomers in a group and its listed value for ΔI^2 in Table 2. We clearly find the same behavior for the values of ΔI^2 if the value of N is increased as in the case of the subset of deuterated derivatives of σ-[4]helicene. For low values of N there is a decrease of ΔI^2 as N increases. At $N = 6$, however, there is the same anomaly as in the case of the subset of deuterated derivatives of σ-[4]helicene where the value of ΔI^2 is increased (or stagnates) compared to the case for which $N = 5$. From the conclusions of section 5.2, we may assume that this effect is an artifact and that if we were able to analyze the complete set of deuterated derivatives of σ-[10]helicene, we would find a generally uniform decrease of the values of ΔI^2 with an increasing value of N.

We conclude that an increased molecular size has a negative influence on the capabilities of ROA spectroscopy. For $N = 5$ and a value of 20 cm^{-1} chosen for the fwhm, it is possible to determine the absolute configuration of all chiral centers in the deuterated derivatives of σ-[4]helicene. This is not possible for σ-[10]helicene. Furthermore, we understand that $N = 4$ is an upper bound estimate for the number of chiral centers for which the absolute configuration can be detected by ROA spectroscopy for a molecule similar to σ-[10]helicene.

5.4. Analysis of Different Substituent Types. We now investigate how different substituents influence the capability of ROA spectroscopy in determining the absolute configuration of chiral centers. For this purpose we analyze singly substituted derivatives of both scaffold molecules chosen for this work. The substituents are deuterium atoms, fluorine atoms, and methyl groups. The derivatives are always substituted in the same positions since we are interested in the effect of the different substituents only. The position of substitution is either 10 or 11 in the case of σ-[4]helicene and either 22 or 23 in the case of σ-[10]helicene. By this analysis we aim at finding a general rule for assessing the capability of ROA spectroscopy in detecting the absolute configuration of stereoisomers with respect to the functional groups forming the molecule under analysis.

Before we start the investigation, we study how the three different substituents affect the spectrum of the unsubstituted scaffold molecule. The effect on bending modes is negligible, since the stretching vibrations are the ones mainly affected by the substitution. A C−H stretching mode (3000−2840 cm^{-1} [83]) is changed into a C−D stretching mode (2200−2080 cm^{-1}). It should be noted that the shifted mode will be

Table 3. Results of Differently Substituted Derivatives Generated from σ-[10]Helicene and σ-[4]Helicene[a]

			σ-[10]helicene					σ-[4]helicene				
			b = 1800 cm^{-1}		b = 3600 cm^{-1}			b = 1800 cm^{-1}		b = 3600 cm^{-1}		
N	fwhm	S	ΔI^2	Dst	ΔI^2	Dst	Inc	ΔI^2	Dst	ΔI^2	Dst	Inc
1	20	F	0.016	yes	0.023	yes	0.007	0.008	yes	0.012	yes	0.004
1	20	M	0.013	yes	0.023	yes	0.010	0.008	yes	0.015	yes	0.007
1	20	D	0.015	yes	0.025	yes	0.010	0.006	yes	0.017	yes	0.011
1	7	F	0.043	yes	0.056	yes	0.013	0.016	yes	0.024	yes	0.008
1	7	M	0.035	yes	0.047	yes	0.012	0.017	yes	0.028	yes	0.011
1	7	D	0.047	yes	0.058	yes	0.011	0.015	yes	0.028	yes	0.013

[a]The three substituents (S) are denoted as "D" for deuterium atoms, "F" for fluorine atoms, and "M" for methyl groups. Additionally, it is stated whether the spectra of the considered pair of derivatives are distinguishable from one another (Dst) and by how much ΔI^2 (Å^4 amu^{-1}) increases (Inc) if the upper limit of vibrational frequencies considered b is changed from 1800 to 3600 cm^{-1}. The results are listed for both fwhm values (cm^{-1}) analyzed.

dx.doi.org/10.1021/jp303428f | J. Phys. Chem. A 2012, 116, 5410−5419

located in a part of the spectrum where no other modes are present. When we use fluorine atoms, a C−H stretching mode is changed into a C−F stretching mode (1400−1000 cm^{-1}). Here, the shifted mode is located in a part of the spectrum where it is likely that other modes are present. For deuterium atoms this new mode is only included in the analysis if b = 3600 cm^{-1}. The new C−C bond in the methyl derivatives affects the scaffold vibrations.

Table 3 lists the result obtained from the analysis of the three different substituents. The corresponding ROA spectra are presented in the Supporting Information. We are especially interested in the increase of the value of ΔI^2 if the value of b is changed from 1800 to 3600 cm^{-1}. This allows us to assess the role of the isolated C−D stretching mode (new signal in a previously empty part of the spectrum) and the C−H stretching modes newly introduced by the methyl groups (new signal in a crowded part of the spectrum).

In Table 3, we notice that the value of ΔI^2 is increased in all cases when the value of b is changed from 1800 to 3600 cm^{-1}. The increase is strongest for the deuterated derivatives and smallest for the fluorinated derivatives. The increase of ΔI^2 for the methylated derivatives is in between. From this we see that an increase of the number of signals in general increases the chiral information. If the additional signal is well separated, as for the deuterated derivatives, more of the additional chiral information is accessible. If the additional signals overlap, as for the methylated derivatives, then not all of the new chiral information can be accessed. Hence a certain balance is required between the number of signals and their distinction from the rest of the spectrum such that ROA spectroscopy can access as much chiral information as possible. Now, we also better understand the reason for the negative effect of an increased molecular size on the capability of ROA spectroscopy in detecting the absolute configuration of chiral centers. An increased molecular size results in more modes, which may lead to a crowding of similar signals if the increasing size is due to similar functional groups or scaffold patterns. Signals are bound to overlap when a critical molecular size is reached. This critical molecular size depends on the fwhm.

6. CONCLUSIONS

The different parts of our analysis provide insights into the question of how many chiral centers can be detected by ROA spectroscopy. All chiral centers in all deuterated derivatives of σ-[4]helicene can be detected by ROA spectroscopy if derivatives with an equal number of chiral centers are compared. This is, however, not the case for σ-[10]helicene. Here, even with the restriction of fixed positions of the chiral centers in the scaffold molecule, at most four chiral centers can be detected if the full width at half-maximum is chosen to be 20 cm^{-1}. The increased number of vibrational modes, due to the increased number of atoms in similar functional groups, causes overlap and cancellation of signals. However, if the resolution is increased, i.e., if fwhm is changed from 20 to 7 cm^{-1}, the chiral centers of deuterated derivatives of σ-[10]helicene can all be distinguished by ROA spectroscopy.

Clearly, the number of chiral centers which can be detected by ROA spectroscopy is defined by the distribution and density of vibrational modes with respect to the vibrational frequency. If there are more vibrational frequencies present in a certain region of the ROA spectrum, it is less likely that they can help to distinguish a given spectrum from the spectrum of other stereoisomers since there will be significant canceling and overlapping of signals. Well-separated signals, however, are more suited for distinguishing a spectrum from other spectra. Moreover, the number of potential stereoisomers has a clear influence on the values of ΔI^2. Not unexpectedly, a large number of stereoisomers results in a low value of ΔI^2. The only case for which this is different is the group of five times deuterated derivatives of σ-[4]helicene with a fwhm of 7 cm^{-1} in comparison to the four times deuterated derivatives.

Finally, we demonstrated that there is no localization of the chiral information within a small range of vibrational frequencies. The best examples are the four and five times deuterated derivatives of σ-[10]helicene at a fwhm of 20 cm^{-1}. Notably, the C−D stretching vibration is not contained in the ROA spectra for an upper integration bound of b = 1800 cm^{-1}, and still the spectra of the four times deuterated derivatives can be distinguished even for this value of b. For the five times deuterated derivatives it is not possible to distinguish all spectra from one another, independent of the value of b. Hence, it is not important whether the C−D stretching mode is included in the analysis or not. This can be explained by the fact that up to 1800 cm^{-1} vibrational modes exist which are largely delocalized over the whole molecular structure. Furthermore, not only the chemical environment at the chiral center itself is important when detecting chiral centers with ROA spectroscopy, but also the extended surrounding of the chiral center is important. However, the number of chiral centers which can be distinguished by ROA spectroscopy appears not to be directly defined by the structures of the stereoisomers analyzed. Chemical similarity does not necessarily correlate with spectral similarity: the pair of structures which resulted in the lowest value of ΔI^2 differed in more than one position of deuteration for both scaffold molecules.

It should be noted that the stereoisomers studied in this work can be expected to be very challenging for ROA spectroscopy. That is, not only have all the chiral centers the same chemical environment; also the scaffold molecule itself is C_2-symmetric. This increases the density of vibrational modes in populated parts in the ROA spectra. Obviously, chiral centers with different chemical environments can be detected more easily by ROA spectroscopy due to the vibrational modes being spread over a wider range of vibrational frequencies. However, typical natural products with more than a dozen chiral centers also contain very similar structural elements leading to crowded regions in the vibrational spectra.

■ ASSOCIATED CONTENT

Supporting Information

Listings of Cartesian coordinate files of optimized structures; Tables I−III listing substitution patterns which resulted in a minimal value of ΔI^2 for deuterated derivatives; Table IV listing equivalent hydrogen atoms of the two scaffold molecules; Figures 1−78 showing plots of ROA spectra; Figure 79 illustrating substitution pattern notation. This material is available free of charge via the Internet at http://pubs.acs.org.

■ AUTHOR INFORMATION

Corresponding Author

*E-mail: markus.reiher@phys.chem.ethz.ch.

Notes

The authors declare no competing financial interest.

■ ACKNOWLEDGMENTS

This work has been supported by the Swiss National Science Foundation SNF (Project 200020-132542/1). Parts of this work were presented in August 2011 at the 47th Symposium for Theoretical Chemistry STC 2011 in Sursee, Switzerland.

■ REFERENCES

(1) Leitereg, T. J.; Guadagni, D. G.; Harris, J.; Mon, T. R.; Teranishi, R. *J. Agric. Food Chem.* **1971**, *19*, 785−787.
(2) Gaich, T.; Baran, P. S. *J. Org. Chem.* **2010**, *75*, 4657−4673.
(3) Polavarapu, P. L. *Chem. Rec.* **2007**, *7*, 125−136.
(4) Barron, L. D. *Molecular Light Scattering and Optical Activity*, 2nd ed.; Cambridge Univeristy Press: Cambridge, U.K., 2004.
(5) Barron, L. D.; Buckingham, A. D. *Chem. Phys. Lett.* **2010**, *492*, 199−213.
(6) Barron, L. D.; Buckingham, A. D. *Annu. Rev. Phys. Chem.* **1975**, *26*, 381−396.
(7) Bhagavantam, S.; Venkateswaran, S. *Nature* **1930**, *125*, 237−238.
(8) Barron, L. D.; Bogaard, M. P.; Buckingham, A. D. *J. Am. Chem. Soc.* **1973**, *95*, 603−605.
(9) Barron, L. D.; Buckingham, A. D. *Mol. Phys.* **1971**, *20*, 1111−1119.
(10) Hug, W.; Kint, S.; Bailey, G. F.; Scherer, J. R. *J. Am. Chem. Soc.* **1975**, *97*, 5589−5590.
(11) Ruud, K.; Thorvaldsen, A. J. *Chirality* **2009**, *21*, E54−E67.
(12) Nafie, L. A.; Keiderling, T. A.; Stephens, P. J. *J. Am. Chem. Soc.* **1976**, *98*, 2715−2723.
(13) Hecht, L.; Barron, L. D.; Hug, W. *Chem. Phys. Lett.* **1989**, *158*, 341−344.
(14) Blanch, E. W.; Robinson, D. J.; Hecht, L.; Syme, C. D.; Nielsen, K.; Barron, L. D. *J. Gen. Virol.* **2002**, *83*, 241−246.
(15) Lamparska, E.; Liégeois, V.; Quinet, O.; Champagne, B. *ChemPhysChem* **2006**, *7*, 2366−2376.
(16) Liégeois, V.; Jacob, C. R.; Champagne, B.; Reiher, M. *J. Phys. Chem. A* **2010**, *144*, 7198−7212.
(17) Merten, C.; Barron, L. D.; Hecht, L.; Johannessen, C. *Angew. Chem.* **2011**, *123*, 10149−10152.
(18) Herrmann, C.; Ruud, K.; Reiher, M. *Chem. Phys.* **2008**, *343*, 200−209.
(19) Herrmann, C.; Ruud, K.; Reiher, M. *ChemPhysChem* **2006**, *7*, 2189−2196.
(20) Šebek, J.; Kapitán, J.; Šebestík, J.; Baumruk, V.; Bouř, P. *J. Phys. Chem. A* **2009**, *113*, 7760−7768.
(21) Bouř, P.; Kapitán, J.; Baumruk, V. *J. Phys. Chem. A* **2001**, *105*, 6362−6368.
(22) Jacob, C. R.; Luber, S.; Reiher, M. *ChemPhysChem* **2008**, *9*, 2177−2180.
(23) Hudecová, J.; Kapitán, J.; Baumruk, V.; Hammer, R. P.; Keiderling, T. A.; Bouř, P. *J. Phys. Chem. A* **2010**, *114*, 7642−7651.
(24) Kapitán, J.; Baumruk, V.; Kopecký, V.; Bouř, P. *J. Phys. Chem. A* **2006**, *110*, 4689−4696.
(25) Bouř, P.; Sychrovský, V.; Maloň, P.; Hanzliková, J.; Baumruk, V.; Popíšek, J.; Buděšinský, M. *J. Phys. Chem. A* **2002**, *106*, 7321−7327.
(26) Luber, S.; Herrmann, C.; Reiher, M. *J. Phys. Chem. B* **2008**, *112*, 2218−2232.
(27) Luber, S.; Reiher, M. *ChemPhysChem* **2009**, *10*, 2049−2057.
(28) Bouř, P. *J. Comput. Chem.* **2001**, *22*, 426−435.
(29) Luber, S.; Reiher, M. *Chem. Phys.* **2008**, *346*, 212−223.
(30) Luber, S.; Reiher, M. *ChemPhysChem* **2010**, *11*, 1876−1887.
(31) Johannessen, C.; Hecht, L.; Merten, C. *ChemPhysChem* **2011**, *12*, 1419−1421.
(32) Jacob, C. R. *ChemPhysChem* **2011**, *12*, 3291−3306.
(33) Luber, S.; Reiher, M. *J. Phys. Chem. A* **2009**, *113*, 8268−8277.
(34) Macleod, N. A.; Johannessen, C.; Hecht, L.; Barron, L. D.; Simons, J. P. *Int. J. Mass Spectrom.* **2006**, *253*, 193−200.
(35) Kaminský, J.; Kapitán, J.; Baumruk, V.; Bednárová, L.; Bouř, P. *J. Phys. Chem. A* **2009**, *113*, 3594−3601.
(36) Hug, W.; Surbeck, H. *Chem. Phys. Lett.* **1979**, *60*, 186−192.
(37) Hug, W.; Zuber, G.; de Meijere, A.; Khlebnikov, A. F.; Hansen, H.-J. *Helv. Chim. Acta* **2001**, *84*, 1−21.
(38) Fedorovsky, M.; Gerlach, H.; Hug, W. *Helv. Chim. Acta* **2009**, *92*, 1451−1465.
(39) Kapitán, J.; Johannessen, C.; Bouř, P.; Hecht, L.; Barron, L. D. *Chirality* **2009**, *21*, E4−E12.
(40) Cheeseman, J. R.; Shaik, M. S.; Popelier, P. L. A.; Blanch, E. W. *J. Am. Chem. Soc.* **2011**, *133*, 4991−4997.
(41) Bouř, P.; Baumruk, V.; Hanzliková, J. *Collect. Czech. Chem. Commun.* **1997**, *62*, 1384−1395.
(42) Haesler, J.; Schindelholz, I.; Riguet, E.; Bochet, C. G.; Hug, W. *Nature* **2007**, *446*, 526−529.
(43) Pecul, M.; Deillon, C.; Thorvaldsen, A.; Ruud, K. *J. Raman Spectrosc.* **2010**, *41*, 1200−1210.
(44) Drooghaag, X.; Marchand-Brynaert, J.; Champagne, B.; Liégeois, V. *J. Phys. Chem. B* **2010**, *114*, 11753−11760.
(45) Nieto-Ortega, B.; Casado, J.; Blanch, E. W.; Navarette, J. T. L.; Quesada, R.; Ramirez, F. J. *J. Phys. Chem. A* **2011**, *115*, 2752−2755.
(46) Reiher, M.; Liégeois, V.; Ruud, K. *J. Phys. Chem. A* **2005**, *109*, 7567−7574.
(47) Luber, S.; Neugebauer, J.; Reiher, M. *J. Chem. Phys.* **2010**, *132*, 044113.
(48) Hopmann, K. H.; Ruud, K.; Pecul, M.; Kudelski, A.; Dračínský, M.; Bouř, P. *J. Phys. Chem. B* **2011**, *115*, 4128−4137.
(49) Šebestík, J.; Bouř, P. *J. Phys. Chem. Lett.* **2011**, *2*, 498−502.
(50) Yamamoto, S.; Straka, M.; Watarai, H.; Bouř, P. *Phys. Chem. Chem. Phys.* **2010**, *12*, 11021−11032.
(51) Yamamoto, S.; Watarai, H.; Bouř, P. *ChemPhysChem* **2011**, *12*, 1509−1518.
(52) Luber, S.; Reiher, M. *J. Phys. Chem. B* **2010**, *114*, 1057−1063.
(53) Ruud, K.; Helgaker, T.; Bouř, P. *J. Phys. Chem. A* **2002**, *106*, 7448−7455.
(54) Herrmann, C.; Reiher, M. *Top. Curr. Chem.* **2007**, *268*, 85−132.
(55) Shigeki, Y.; Bouř, P. *Collect. Czech. Chem. Commun.* **2011**, *76*, 567−583.
(56) Bieler, N.; Haag, M. P.; Jacob, C. R.; Reiher, M. *J. Chem. Theory Comput.* **2011**, *7*, 1867−1881.
(57) Li, X.; Hopmann, H.; Hudecová, J.; Stensen, W.; Novotná, J.; Urbanová, M.; Svendsen, J.-S.; Bouř, P.; Ruud, K. *J. Phys. Chem. A* **2012**, *116*, 2554−2563.
(58) Hopmann, K. H.; Šebestík, J.; Novotná, J.; Stensen, W.; Urbanová, M.; Svenson, J.; Svendsen, J. S.; Bouř, P.; Ruud, K. *J. Org. Chem.* **2012**, *77*, 858−869.
(59) Ahlrichs, R.; Bär, M.; Häser, M.; Horn, H.; Kölmel, C. *Chem. Phys. Lett.* **1989**, *162*, 165−169.
(60) Becke, A. D. *Phys. Rev. A* **1988**, *38*, 3098−3100.
(61) Perdew, J. P. *Phys. Rev. B* **1986**, *33*, 8822−8824.
(62) Schäfer, A.; Huber, C.; Ahlrichs, R. *J. Chem. Phys.* **1994**, *100*, 5829−5835.
(63) Dunning, T. H., Jr. *J. Chem. Phys.* **1989**, *90*, 1007−1023.
(64) Eichkorn, K.; Treutler, O.; Öhm, H.; Häser, M.; Ahlrichs, R. *Chem. Phys. Lett.* **1995**, *240*, 283−290.
(65) Eichkorn, K.; Treutler, O.; Öhm, H.; Häser, M.; Ahlrichs, R. *Chem. Phys. Lett.* **1995**, *242*, 652−660.
(66) Neugebauer, J.; Reiher, M.; Kind, C.; Hess, B. A. *J. Comput. Chem.* **2002**, *23*, 895−910.
(67) Reiher, M.; Neugebauer, J.; Hess, B. A. *Z. Phys. Chem.* **2003**, *217*, 91−103.
(68) Reiher, M.; Brehm, G.; Schneider, S. *J. Phys. Chem. A* **2004**, *108*, 734−742.
(69) Brehm, G.; Reiher, M.; Schneider, S. *J. Phys. Chem. A* **2002**, *106*, 12024−12034.
(70) Yu, L.; Greco, C.; Bruschi, M.; Rydes, U.; de Goia, L.; Reiher, M. *Inorg. Chem.* **2011**, *50*, 3888−3900.
(71) Neugebauer, J.; Hess, B. A. *J. Chem. Phys.* **2003**, *118*, 7215−7225.
(72) Furche, F.; Rappoport, D. In *Theoretical and Computational Chemistry*; Olivucci, M., Ed., Elsevier: New York, 2005; Vol. *16*; Chapter III, pp 93−128.

(73) Moulton, P. F. *J. Opt. Soc. Am. B* **1986**, *3*, 125−133.
(74) R Development Core Team. *R: A Language and Environment for Statistical Computing*; R Foundation for Statistical Computing: Vienna, Austria, 2011.
(75) Urbanek, S.; Horner, J. *Cairo: R Graphics Device using Cairo Graphics Library for Creating High-Quality Bitmap (PNG, JPEG, TIFF), Vector (PDF, SVG, PostScript) and Display (X11 and Win32) Output*; 2009.
(76) Inkscape: Open Source Scalable Vector Graphics Editor, version 0.48.
(77) Avogadro: An Open-Source Molecular Builder and Visualization Tool, version 1.0.0.
(78) de Meijere, A.; Khlebnikov, A. F.; Kozhushkov, S. I.; Kostikov, R. R.; Schreiner, P. R.; Wittkopp, A.; Rinderspacher, C.; Menzel, H.; Yufit, D. S.; Howard, J. A. K. *Chem.—Eur. J.* **2002**, *8*, 828−842.
(79) Zefirov, N. S.; Kozhushkov, S. I.; Kuznetsova, T. S.; Kokoreva, O. V.; Lukin, K. A.; Ugrak, B. I.; Tratch, S. S. *J. Am. Chem. Soc.* **1990**, *112*, 7702−7707.
(80) de Meijere, A.; Khlebnikov, A. F.; Kozhushkov, S. I.; Yufit, D. S.; Chetina, O. V.; Howard, J. A. K.; Kurahashi, T.; Miyazawa, K.; Frank, D.; Schreiner, P. R.; Rinderspacher, B. C.; Fujisawa, M.; Yamamoto, C.; Okamoto, Y. *Chem.—Eur. J.* **2006**, *12*, 5697−5721.
(81) Debie, E.; Gussem, E. D.; Dukor, R. K.; Herrebout, W.; Nafie, L. A.; Bultinck, P. *ChemPhysChem* **2011**, *12*, 1439−7641.
(82) Rossi, M.; Blum, V.; Kupser, P.; von Helden, G.; Bierau, F.; Pagel, K.; Meijer, G.; Scheffler, M. *J. Phys. Chem. Lett.* **2010**, *1*, 3465−3470.
(83) Pretsch, E.; Bühlmann, P.; Affolter, C.; Badertscher, M. *Spektroskopische Daten zur Strukturaufklärung organischer Verbindungen*, 4th ed.; Springer: Berlin, 2001.